J Physiol 587.11 (2009) pp 2537–2553

Ca^{2+} sensitization via phosphorylation of myosin phosphatase targeting subunit at threonine-855 by Rho kinase contributes to the arterial myogenic response

Rosalyn P. Johnson[1], Ahmed F. El-Yazbi[1], Kosuke Takeya[2], Emma J. Walsh[1], Michael P. Walsh[2] and William C. Cole[1]

The Smooth Muscle Research Group, Departments of [1]Physiology & Pharmacology and [2]Biochemistry & Molecular Biology, Faculty of Medicine, University of Calgary, Calgary, Alberta, Canada

Ca^{2+} sensitization has been postulated to contribute to the myogenic contraction of resistance arteries evoked by elevation of transmural pressure. However, the biochemical evidence of pressure-induced increases in phosphorylated myosin light chain phosphatase (MLCP) targeting subunit 1 (MYPT1) and/or 17 kDa protein kinase C (PKC)-potentiated protein phosphatase 1 inhibitor protein (CPI-17) required to sustain this view is not currently available. Here, we determined whether Ca^{2+} sensitization pathways involving Rho kinase (ROK)- and PKC-dependent phosphorylation of MYPT1 and CPI-17, respectively, contribute to the myogenic response of rat middle cerebral arteries. ROK inhibitors (Y27632, 0.03–10 μmol l^{-1}; H1152, 0.001–0.3 μmol l^{-1}) and PKC inhibitors (GF109203X, 3 μmol l^{-1}; Gö6976; 10 μmol l^{-1}) suppressed myogenic vasoconstriction between 40 and 120 mmHg. An improved, highly sensitive 3-step Western blot method was developed for detection and quantification of MYPT1 and CPI-17 phosphorylation. Increasing pressure from 10 to 60 or 100 mmHg significantly increased phosphorylation of MYPT1 at threonine-855 (T855) and myosin light chain (LC_{20}). Phosphorylation of MYPT1 at threonine-697 (T697) and CPI-17 were not affected by pressure. Pressure-evoked elevations in MYPT1-T855 and LC_{20} phosphorylation were reduced by H1152, but MYPT1-T697 phosphorylation was unaffected. Inhibition of PKC with GF109203X did not affect MYPT1 or LC_{20} phosphorylation at 100 mmHg. Our findings provide the first direct, biochemical evidence that a Ca^{2+} sensitization pathway involving ROK-dependent phosphorylation of MYPT1 at T855 (but not T697) and subsequent augmentation of LC_{20} phosphorylation contributes to myogenic control of arterial diameter in the cerebral vasculature. In contrast, suppression of the myogenic response by PKC inhibitors cannot be attributed to block of Ca^{2+} sensitization mediated by CPI-17 or MYPT1 phosphorylation.

(Received 19 December 2008; accepted after revision 30 March 2009; first published online 9 April 2009)

Corresponding author W. C. Cole: The Smooth Muscle Research Group, Department of Physiology and Pharmacology, Faculty of Medicine, University of Calgary, 3330 Hospital Drive N.W., Calgary, Alberta, Canada T2N 4N1.
Email: wcole@ucalgary.ca

Abbreviations BPB, bromophenol blue; $[Ca^{2+}]_i$, cytosolic Ca^{2+} level; CPI-17, 17 kDa protein kinase C-potentiated protein phosphatase 1 inhibitor protein; DTT, dithiothreitol; E_m, membrane potential; HRP, horseradish peroxidase; LC_{20}, 20 kDa myosin light chain subunit; MLCK, myosin light chain kinase; MLCP, myosin light chain phosphatase; MYPT1, myosin light chain phosphatase targeting subunit 1; PdBu, phorbol 12,13-dibutyrate; PKC, protein kinase C; Phos-tag SDS-PAGE, SDS-PAGE with polyacriylamide-bound Mn^{2+} tag; RCA, rat middle cerebral artery; ROK, Rho kinase; TBS, Tris-buffered saline; TBST, TBS containing 0.02% Tween-20; TCA, trichloroacetic acid; TEMED, *N*,*N*,*N*′,*N*′-tetramethyl ethylenediamine; UTP, uridine 5′-triphosphate; VGCCs, voltage-gated Ca^{2+} channels.

The ability of resistance arteries to constrict in response to increased transmural pressure and to dilate to pressure reduction is referred to as the myogenic response. This mechanism is an important determinant of peripheral vascular resistance, blood pressure and regional blood flow control in several vascular beds, including cerebral vasculature (Davis & Hill 1999). Although the myogenic response has been recognized for more than

DOI: 10.1113/jphysiol.2008.168252

100 years (Bayliss, 1902), our understanding of the basic mechanisms involved in this fundamental physiological mechanism is incomplete.

The myogenic response is known to be an intrinsic property of the vascular smooth muscle cells of resistance arteries and occurs in the absence of endothelial or neuronal input (Davis & Hill, 1999; Hill *et al.* 2001). Myogenic contraction is dependent in part on the level of membrane potential (E_m) of vascular smooth muscle cells, since the major source of contractile Ca^{2+} influx occurs through voltage-gated Ca^{2+} channels (VGCCs) (Davis & Hill, 1999; Hill *et al.* 2001, 2006). A current working hypothesis holds that the myogenic response results from: (1) pressure-induced depolarization of E_m owing to activation of non-selective cation channels (and/or chloride and VGCCs), (2) voltage-dependent activation of VGCCs, (3) a rise in cytosolic Ca^{2+} level ($[Ca^{2+}]_i$), (4) Ca^{2+}-dependent activation of myosin light chain kinase (MLCK), (5) phosphorylation of the 20 kDa myosin light chain subunit (LC_{20}), (6) initiation of cross-bridge cycling, and (7) force generation (Zou *et al.* 1995, 2000; Davis & Hill, 1999; Hill *et al.* 2001, 2006).

Several lines of evidence suggest, however, that mechanisms in addition to changes in membrane potential and $[Ca^{2+}]_i$ may also contribute to force generation in the myogenic response (D'Angelo *et al.* 1997; van Bavel *et al.* 2001; Lagaud *et al.* 2002; Osol *et al.* 2002; Gokina *et al.* 2005). Marked changes in E_m and $[Ca^{2+}]_i$ accompany myogenic contraction of cerebral arteries to pressures $< \sim$60 mmHg (Osol *et al.* 2002). However, neither parameter changed appreciably between 60 and 140 mmHg despite increased force generation to maintain diameter constant. Similarly, steady-state constriction of hamster cheek pouch arterioles was greater for larger pressure steps, but the change in $[Ca^{2+}]_i$ was similar (D'Angelo *et al.* 1997). Myogenic contraction has also been observed in elevated external $[K^+]$ solution, a manipulation that clamps E_m at a depolarized level and precludes changes in Ca^{2+} entry via VGCCs (Lagaud *et al.* 2002). The myogenic response is suppressed by inhibition of PKC activity or suppression of ROK with Y27632 or dominant-negative mutants of RhoA and ROK (van Bavel *et al.* 2001; Lagaud *et al.* 2002; Schubert *et al.* 2002; Yeon *et al.* 2002; Bolz *et al.* 2003; Nakamura *et al.* 2003; Jarajapu & Knot, 2005; Dubroca *et al.* 2005, 2007; Gokina *et al.* 2005). For example, Y27632 caused vasodilatation in high external $[K^+]$ or following α-toxin permeabilization without a change in intracellular $[Ca^{2+}]_i$ (Lagaud *et al.* 2002; Gokina *et al.* 2005). Taken together, these findings have been interpreted to indicate that ROK- and/or PKC-dependent mechanisms of Ca^{2+} sensitization contribute to the myogenic response (Schubert *et al.* 2008) in a manner similar to agonist-induced contraction of smooth muscle (Somlyo & Somlyo, 2003; Swärd *et al.* 2003; Hirano, 2007).

Ca^{2+} sensitization is the phenomenon whereby agonists evoke contraction of smooth muscle with little or no rise in $[Ca^{2+}]_i$ by modifying the balance between MLCK and myosin light chain phosphatase (MLCP) activity (Somlyo & Somlyo, 2003). The extent of LC_{20} phosphorylation and subsequent force generation is determined by the relative activities of MLCK and MLCP. Agonists that activate $G_{12/13}$-coupled receptors induce sensitization through the activation of ROK by the small GTPase RhoA (Somlyo & Somlyo, 2003; Swärd *et al.* 2003; Hirano, 2007). ROK phosphorylates MLCP targeting subunit 1 (MYPT1) at threonine-697 (T697) and/or threonine-855 (T855) (and possibly CPI-17; Hirano, 2007), in a tissue-dependent manner resulting in a suppression of MLCP activity (Feng *et al.* 1999; Velasco *et al.* 2002; Murányi *et al.* 2005). Ca^{2+} sensitization is also induced by PKC activation following G_q-coupled receptor occupancy and subsequent phosphorylation of CPI-17 at threonine-38 that results in a 1000-fold increase in the inhibitory effect of CPI-17 on MLCP (Hayashi *et al.* 2001). The decrease in MLCP activity evoked by both signalling pathways shifts the MLCK–MLCP balance in favour of MLCK-dependent phosphorylation of LC_{20}, resulting in greater force generation at a given $[Ca^{2+}]_i$; i.e. a leftward shift in the force *versus* $[Ca^{2+}]_i$ relation (Somlyo & Somlyo, 2003; Swärd *et al.* 2003).

If ROK- and/or PKC-mediated Ca^{2+} sensitization contribute to the myogenic response, MYPT1 and/or CPI-17 phosphorylation would be expected to increase coincidently with increased phospho-LC_{20}, force generation and a leftward shift in the force *versus* $[Ca^{2+}]_i$ relation. Significantly, at present: (1) there is no evidence that elevations in transmural pressure evoke an increase in MYPT1 or CPI-17 phosphorylation in resistance arteries, and (2) in the only study to directly test for sensitization over the physiological range of $[Ca^{2+}]_i$ using pressurized, α-toxin-permeabilized arteries, no change in the force *versus* $[Ca^{2+}]_i$ relation was apparent between 0 and 80 mmHg (McCarron *et al.* 1997). Indeed, previous studies have relied exclusively on surrogate, indirect markers of changes in Ca^{2+} sensitivity (Schubert *et al.* 2008), such as alterations in the relationship between arterial diameter and bulk $[Ca^{2+}]_i$ assessed with Fura-2 (e.g. D'Angelo *et al.* 1997). In the absence of direct evidence of Ca^{2+} sensitization, it is impossible to discount the possibility that suppression of myogenic contraction owing to inhibition of ROK- or PKC-signalling results from an interference with other cellular mechanisms that have been implicated in the myogenic response. For example, ROK and PKC are well known to alter smooth muscle L-type Ca^{2+}, non-selective cation and K^+ channel activity, modify Ca^{2+} handling, regulate cross-bridge cycling (via calponin or caldesmon) and/or affect actin cytoskeleton rearrangement (Cipolla & Osol, 1998; Jin *et al.* 2000; Kaneko *et al.* 2000; Morgan & Gangopadhyay,

2001; Ghisdal *et al.* 2003; Wier & Morgan, 2003; Shabir *et al.* 2004; Luykenaar *et al.* 2004; Wilson *et al.* 2005; Gerthoffer, 2005; Villalba *et al.* 2008).

Obtaining biochemical evidence of Ca^{2+} sensitization in the myogenic response has been problematic (Davis & Hill, 1999; Schubert *et al.* 2002, 2008). Routine measurement of MYPT1, CPI-17 and LC_{20} phosphorylation in resistance arteries has not been possible because of the small size of the vessels. For example, the segments of rat middle cerebral arteries (RCAs) used in many pressure arteriography studies are typically 0.5–1.0 mm long and 0.1–0.2 mm in diameter with a wall thickness of 2–5 smooth muscle cells. These segments yield less than 1 μg protein and only trace quantities of MYPT1, CPI-17 and LC_{20} that cannot be detected by standard Western blotting techniques. Accurate quantification of phospho-MYPT1 and phospho-CPI-17 in myogenic arteries therefore requires the development of a method with higher sensitivity, as was employed to measure LC_{20} phosphorylation in 20 μm diameter renal afferent arterioles (Takeya *et al.* 2008).

In this study, we tested the hypothesis that Ca^{2+} sensitization mechanisms mediated by MYPT1 and CPI-17 phosphorylation by ROK and PKC, respectively, contribute to the myogenic response of RCAs. We employed a 3-step Western blot method to quantify phospho-MYPT1, phospho-CPI-17 and phospho-LC_{20} at varied intra-luminal pressure. Our data provide the first direct, biochemical evidence that elevations in pressure elicit a ROK-dependent phosphorylation of MYPT1 at T855, leading to an augmentation of LC_{20} phosphorylation that contributes to force generation in the myogenic response.

Methods

Ethical approval

Male Sprague–Dawley rats (250–275 g; Charles River, Montréal, Quebec, Canada) were maintained and killed by halothane inhalation and exsanguination according to the standards of the Canadian Council on Animal Care and a protocol reviewed by the Animal Care Committee of the Faculty of Medicine, University of Calgary. A total of 95 rats were employed.

Intact cerebral arterial pressure myography

The brain was carefully removed and placed in ice-cold Krebs solution containing (in mmol l^{-1}): NaCl 120, $NaHCO_3$ 25, KCl 4.8, NaH_2PO_4 1.2, $MgSO_4$ 1.2, glucose 11, $CaCl_2$ 1.8 (pH 7.4 when aerated with 95% air–5% CO_2). Left and right middle cerebral arteries (RCAs) were removed from the brain, dissected free of the surrounding tissue and cut into 2 mm segments in preparation for arterial pressure myography, as previously described (Plane *et al.* 2005; Chen *et al.* 2006). Briefly, cerebral arteries were mounted in an arteriograph chamber attached to a pressure myograph (Living Systems, Burlington, VT, USA) for measurement of arterial diameter with an automated edge detection system (IonOptix, Milton, MA, USA). Endothelial cells were removed from all arteries by briefly passing a stream of air through the vessel lumen and confirmed by loss of vasodilatation to 10 μmol l^{-1} bradykinin. Arteries were allowed to warm to 37°C for 30 min in Krebs solution, then pressurized to 60 mmHg and allowed to develop active tone over 30–45 min. All arteries were subjected to two 5 min pressure steps from 20 to 80 mmHg to ensure development of stable pressure-dependent myogenic constriction. Vessels that exhibited leaks and/or did not exhibit stable constriction to pressure were discarded. After development and stabilization of myogenic constriction, pressure was reduced to 10 mmHg for 10 min, and the vessels were then subjected to pressure protocol 1, 2 or 3.

Pressure protocol 1. Concentration-dependent effect of ROK inhibitors on pressure-induced constriction was determined by increasing pressure from 10 to 100 mmHg allowing a stable level of myogenic tone to develop (~5 min) and then applying increasing concentrations of ROK inhibitor (Y27632, 0.03–10 μmol l^{-1}; H1152, 1–3000 nmol l^{-1}) in a cumulative manner to the superfusate, with each new concentration applied after stabilization of the diameter in response to the previous application (typically 10 min for Y27632 and 5 min for H1152). Ca^{2+}-free Krebs solution (zero $[Ca^{2+}]_o$) containing 1.0 mmol l^{-1} EGTA and 10 μmol l^{-1} nitrendipine was used to determine the maximally relaxed arterial diameter at 100 mmHg.

Pressure protocol 2. The effect of ROK and PKC inhibitors on myogenic tone over a range of pressures was determined by subjecting vessels to three series of pressure steps from 10 to 120 mmHg in 20 mmHg increments. The first series was applied in normal Krebs solution (Control). Pressure was then reduced to 10 mmHg and H1152 (0.3 μmol l^{-1}), Y27632 (1 μmol l^{-1}), GF109203X (3 μmol l^{-1}) or Gö6976 (10 μmol l^{-1}) was added to the superfusate before a second series of pressure steps. Pressure was then reduced to 10 mmHg again and ROK or PKC inhibitor solution replaced with zero Ca^{2+} Krebs solution prior to a third series of pressure steps to determine the passive diameter of the artery at each pressure. Active myogenic constriction was defined as the difference at each pressure between arterial diameter in zero $[Ca^{2+}]_o$ *versus* normal Krebs solution or in the presence of ROK- or PKC-inhibitor solution.

Pressure protocol 3. Analysis of phospho-MYPT1 and phospho-LC_{20} was accomplished using flash-frozen vessels following a pressure protocol involving two 5 min steps to 80 mmHg and a 10 min equilibration at 10 mmHg, prior to 10 min steps to 10, 60 or 100 mmHg. The final steps to 10, 60 and 100 mmHg were of 3 min duration in the CPI-17 experiments. CPI-17 was also assessed after 0.5 min at 100 mmHg in three experiments. In some MYPT1 experiments, 300 nmol l^{-1} H1152 was added to the superfusate after ∼5 min (i.e. after a stable arterial diameter was achieved). Arteries were flash-frozen in an ice-cold mixture of 10% trichloroacetic acid (TCA) and 10 mmol l^{-1} dithiothreitol (DTT) in acetone. Arteries were washed in ice-cold acetone containing 10 mmol l^{-1} DTT and lyophilized overnight. Prior to protein extraction, the cannulated ends of the vessels were dissected from the lyophilized vessel segment and discarded to avoid including tissue that was not subjected to the test pressures.

Protein extraction

For protein extraction, 400 μl of sample buffer (4% SDS, 100 mmol l^{-1} DTT, 10% glycerol, 0.01% bromophenol blue (BPB), 60 mmol l^{-1} Tris-HCl, pH 6.8) was added to 4–6 pooled cerebral vessels (∼0.5 mm each in length) per experimental group. Samples were heated at 95°C for 10 min and rotated end-over-end overnight at 4°C prior to electrophoresis. Multiple freeze/thaw cycles were avoided to limit protein degradation. Extract from a single vessel segment (0.5–1 mm) was sufficient to permit quantification of MYPT1, CPI-17 or LC_{20} phosphorylation by Western blotting, but a minimum of three vessels was required for simultaneous detection of changes in all three phosphoproteins and, to ensure robust detection, we chose to pool 4–6 vessel segments. A further five LC_{20} blots were performed using samples derived from five individual vessels to ensure that the changes identified using pooled samples were identical to those in individual segments. No difference was apparent and these additional data were also included in the determination of the mean change in phospho-LC_{20} with pressure.

Measurement of LC_{20} phosphorylation

Unphosphorylated and monophosphorylated LC_{20} were separated by SDS-PAGE with polyacrylamide-bound Mn^{2+} tag (Phos-tag SDS-PAGE) as previously described (Takeya *et al.* 2008) with the following modifications: the stacking gel was composed of 4.38% acrylamide, 0.12% *N*,*N*′-methylenebisacrylamide, 0.1% SDS, 125 mmol l^{-1} Tris-HCl pH 6.8, 0.1% ammonium persulfate and 0.17% *N*,*N*,*N*′,*N*′-tetramethyl ethylenediamine (TEMED). The resolving gel was composed of 12.18% acrylamide, 0.32% *N*,*N*′-methylenebisacrylamide, 50 μmol l^{-1} Phos-tag acrylamide (NARD Institute Ltd, Japan), 100 μmol l^{-1} $MnCl_2$, 0.1% SDS, 375 mmol l^{-1} Tris-HCl pH 8.8, 0.05% ammonium persulfate and 0.07% TEMED. Electrophoresis was performed in 0.1% SDS, 25 mmol l^{-1} Tris, 192 mmol l^{-1} glycine at 30 mA (∼1.5 h). After electrophoresis, the gel was soaked in transfer buffer (25 mmol l^{-1} Tris, 192 mmol l^{-1} glycine, 10% methanol) containing 2 mmol l^{-1} EDTA for 15 min, and then in transfer buffer without EDTA for 15 min. Proteins were transferred to PVDF membrane (0.2 μm pore size) overnight at 27 V at 4°C. The following steps were performed at room temperature unless otherwise indicated. Blotted membranes were washed in PBS for 5 min. LC_{20} was cross-linked and fixed on the membrane by soaking in 0.5% glutaraldehyde in PBS for 45 min. After washing in Tris-buffered saline (TBS; 137 mmol l^{-1} NaCl, 3 mmol l^{-1} KCl, 20 mmol l^{-1} Tris-HCl pH 7.5), the membrane was blocked with 0.5% I-Block (Tropix, Bedford, MA, USA) in TBS containing 0.02% Tween-20 (TBST) for 1.5 h. To enhance detection sensitivity, the 3-step Western blot protocol was used to detect LC_{20} from cerebral vessels, and was carried out as follows: all forms of LC_{20} (unphosphorylated and monophosphorylated) were detected using rabbit anti-LC_{20} antibody (1 : 1000 dilution) incubated for 2 h in TBST (0.1%). Membranes were washed in TBST (0.02%), incubated in TBST (0.1%) containing biotin-conjugated goat anti-rabbit IgG (1 : 40 000 dilution) for 1 h, washed again in TBST (0.02%), and incubated for 30 min in TBST (0.1%) containing horseradish peroxidase (HRP)-conjugated streptavidin (1 : 200 000 dilution). Membranes were then washed in TBST (0.02%) and HRP was detected with SuperSignal West Femto reagent (Pierce, Nepean, ON, Canada). The emitted light was detected and quantified with a chemiluminescence imaging analyser (LAS3000mini, Fujifilm Canada, Mississauga, ON, Canada). Obtained images were analysed with Multi Gauge v3.0 software (Fujifilm).

Measurement of MYPT1 phosphorylation

Extracted proteins were separated by SDS-PAGE at 35 mA for 3.5 h using a large-format, 20-slot, 1.5 mm thick, 10% polyacryamide gel. Following electrophoresis, the gel was cut at the 55 kDa molecular mass marker. The low molecular mass proteins were stained with Coomassie Brilliant Blue-R250 to permit quantification of actin. The high molecular mass proteins were transferred to a 0.2 μm nitrocellulose membrane at 100 V for 2 h, in transfer buffer containing 25 mmol l^{-1} Tris-HCl, 192 mmol l^{-1} glycine, 1% SDS and 20% methanol. Membranes were stained with 0.5% Ponceau S in 5% acetic acid for 5 min to fix transferred proteins to the membrane, rinsed in distilled water and dried overnight prior to Western

blotting. Western blotting for phosphorylated MYPT1 was carried out as described for LC_{20} with the following modifications: in the 3-step Western blot protocol, MYPT1 phosphorylated at T697 and T855 was detected using phosphospecific rabbit polyclonal antibodies (1 : 1000 dilution). In the 2-step Western blot protocol, the blocking solution was 5% skimmed milk in TBST (0.05%) and the secondary antibody (HRP-conjugated goat anti-rabbit IgG) was incubated in TBST (0.1%) (1 : 2000 dilution) for 1 h.

Measurement of CPI-17 phosphorylation

Tissues from myograph experiments were extracted in the protein extraction buffer overnight at 4°C as indicated above. Samples were separated by Phos-tag SDS-PAGE as described for LC_{20}. Gels were equilibrated in transfer buffer (10 mmol l^{-1} 3-[cyclohexylamino]-1-propanesulfonic acid (CAPS)-NaOH pH 11, 15% methanol) containing 2 mmol l^{-1} EDTA and proteins were transferred to PVDF membranes at 100 V for 1 h at 4°C. After washing with PBS, the membranes were fixed in 0.5% glutaraldehyde in PBS for 45 min, then washed twice with TBS. The membranes were blocked by 1% enhanced chemiluminescence (ECL) advanced blocking reagent (GE Healthcare) in TBST (0.1%) using SNAP i.d. system (Millipore). Membranes were incubated at 4°C overnight with rabbit polyclonal anti-CPI-17 (1 : 2000 dilution), washed with TBST (0.05%), incubated with biotin-conjugated goat anti-rabbit IgG in TBST (0.1%) for 1 h at room temperature, washed again in TBST (0.05%) and then incubated with HRP-conjugated streptavidin (1 : 100 000) in TBST (0.1%) for 30 min at room temperature prior to exposure to chemiluminescence reagent and quantified as described for LC_{20}.

Materials

All chemicals were purchased from Sigma/VWR unless indicated otherwise. Tween 20 and Coomassie Brilliant Blue-R250 were from Bio-Rad Laboratories (Mississauga, ON, Canada). Rabbit polyclonal antibodies specific for MYPT1 phosphorylated at T697 (anti-MYPT1-pT697) or T855 (anti-MYPT1-pT855) and CPI-17 were purchased from Upstate USA (Charlottesville, VA, USA). The rabbit anti-LC_{20} polyclonal antibody was from Santa Cruz (CA, USA). Biotin-conjugated goat anti-rabbit IgG was from Chemicon International (Billerica, MA, USA), HRP-conjugated goat anti-rabbit secondary antibody and HRP-conjugated streptavidin were from Pierce Biotechnology (Rockford, CT, USA). H1152 was obtained from Calbiochem (San Diego, CA, USA), GF109203X and Gö6976 were from Biomol International (Plymouth Meeting, PA, USA).

Statistical analysis

Where applicable, values are presented as the means ± S.E.M., with n indicating the number of experiments for a given treatment. Statistical differences were determined using Student's t test or repeated measures of ANOVA followed by Bonferroni's *post hoc* test. A level of $P < 0.05$ was considered to be statistically significant.

Results

Highly sensitive method for detection of phosphorylated MYPT1

To permit quantification of MYPT1, CPI-17 and LC_{20} phosphorylation in pressurized RCA, modifications that maximized protein extraction and sensitivity of Western blot detection for each phosphoprotein were identified. MYPT1 extraction was dramatically increased with 4% SDS (rather than 1%) in the sample buffer combined with end-over-end rotation overnight (Supplemental Fig. 1, available online only). This method was also suitable for CPI-17 and LC_{20}. Fixation of MYPT1 to nitrocellulose membranes with 0.5% Ponceau S–5% acetic acid (5 min treatment) improved sensitivity compared to no fixation or fixation with glutaraldehyde (Supplemental Fig. 2). Improved sensitivity was also observed when nitrocellulose was blocked with 0.5% I-Block *versus* other common blocking agents (Supplemental Fig. 3). The greatest improvement in sensitivity was achieved using a 3-step Western blot protocol that incorporated a biotin–streptavidin amplification step. For example, Fig. 1 shows a comparison of a standard 2-step with the 3-step method using a dilution series of uridine 5′-triphosphate (UTP)-stimulated (10 μmol l^{-1}) RCA extracts subjected to SDS-PAGE, transferred to nitrocellulose and phospho-MYPT1 detection using phospho-specific antibodies. The 3-step protocol improved detection sensitivity of phospho-T697- and phospho-T855-MYPT1 by ∼10-fold over a range of dilutions corresponding to pressurized RCA segments of 0.5–3.0 mm length. Phospho-MYPT1 could be quantified on a routine basis using a sample equivalent to a single 0.5 mm segment of pressurized RCA using the 3-step method. Importantly, signal intensity increased in a linear fashion over the dilution range and did not vary when normalized to Coomassie Blue-stained actin to correct for protein loading level (Fig. 2). This method was chosen over normalization to total MYPT1 as it avoided the variable loss of protein introduced by stripping nitrocellulose

membranes prior to re-blotting with pan-MYPT1 antibody.

Inhibition of ROK attenuates myogenic constriction

Y27632 was previously used at 1–10 μmol l^{-1} to study the role of ROK in the myogenic response (van Bavel *et al.* 2001; Lagaud *et al.* 2002; Schubert *et al.* 2002; Yeon *et al.* 2002; Bolz *et al.* 2003; Nakamura *et al.* 2003; Jarajapu & Knot, 2005; Dubroca *et al.* 2005, 2007; Gokina *et al.* 2005). However, it also inhibits PKCδ activity in this concentration range (Eto *et al.* 2001; Wilson *et al.* 2005). Since PKC is implicated in Ca^{2+} sensitization and the myogenic response (Davis & Hill, 1999; Yeon *et al.* 2002; Schubert *et al.* 2008), here we also employed the more potent and selective inhibitor of ROK, H1152 (K_i 0.0016 *vs.* 9.3 μmol l^{-1} for PKC; Sasaki *et al.* 2002). To determine the appropriate concentration of H1152, RCAs were pressurized to 100 mmHg and H1152 was applied in a cumulative manner (Fig. 3). Y27632 was employed in parallel experiments for comparison with the H1152 data. Both inhibitors caused a concentration-dependent vasodilatation, but the IC_{50} value for H1152 was lower than that for Y27632 at 0.02 ± 0.01 compared to 0.44 ± 0.04 μmol l^{-1} (Fig. 3). H1152 and Y27632 at 1.0 and 10 μmol l^{-1}, respectively, induced nearly maximal dilatation (94.2 ± 0.6% and 92.8 ± 1.2%, respectively) to the passive diameter observed in zero $[Ca^{2+}]_o$ solution (no added Ca^{2+}, 1 mmol l^{-1} EGTA and 10 μmol l^{-1} nitrendipine).

Figure 4 shows that Y27632 and H1152 inhibit the myogenic response of RCA. Each vessel segment was subjected to three sequential series of step increases in pressure of 20 mmHg between 20 and 120 mmHg in: (1) control solution, (2) Y27632 (1 μmol l^{-1}; $n = 5$ vessels) or H1152 (0.3 μmol l^{-1}; $n = 5$ vessels) (i.e. to achieve ~80% inhibition of myogenic contraction; Fig. 3) and (3) zero $[Ca^{2+}]_o$ solution. The representative recordings and mean data of Fig. 4 show that steps in pressure to greater than 40 mmHg induced a maintenance or decrease in diameter in control solution, whereas dilatation was observed in Y27632 or H1152. The difference between the passive dilatation in zero $[Ca^{2+}]_o$ and the diameter in control or presence of ROK inhibitor is the extent of active myogenic contraction at each pressure (Fig. 4*C* and *F*). The involvement of ROK is indicated by the attenuated active constriction in Y27632 and H1152 compared to control conditions.

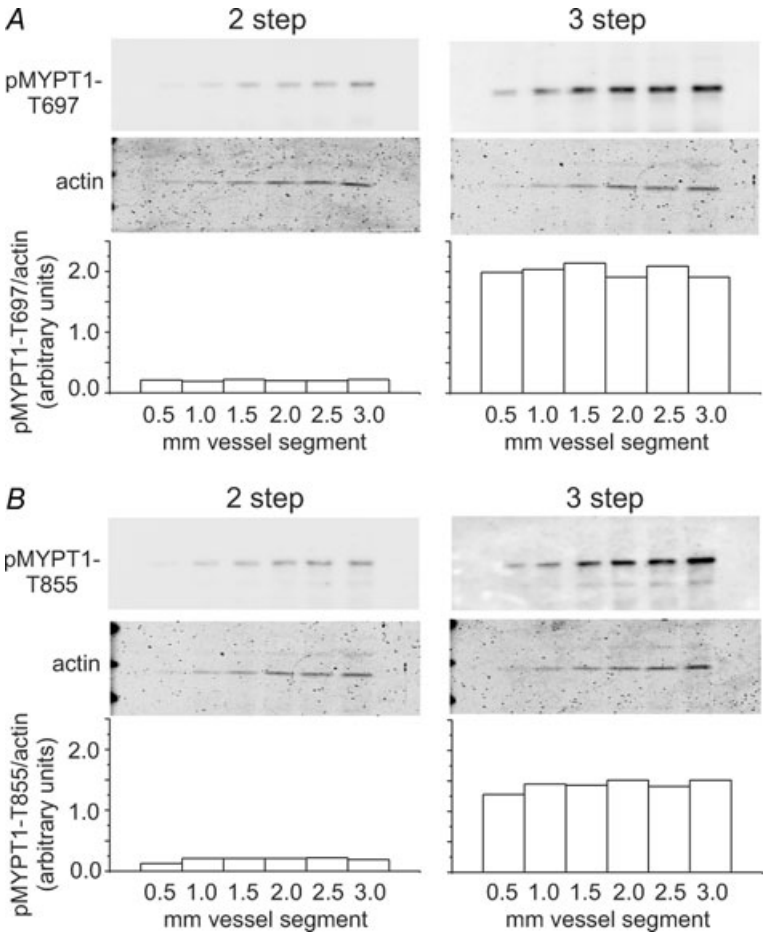

Figure 1. Detection sensitivity of 2-step *versus* enhanced 3-step Western blotting for phospho-MYPT1
A dilution series of UTP-stimulated cerebral artery extract (which approximates the range of signal intensities produced by the indicated number of 200 μm × 500 μm pressurized rat cerebral arterial segments) was subjected to SDS-PAGE and phosphorylation of MYPT1 at T697 (*A*) and T855 (*B*) detected by 2-step and 3-step Western blotting protocols (i.e. simultaneous exposure). Bars show signal intensity of phospho-MYPT1 normalized to Coomassie Blue-stained actin for each dilution detected by the 2-step and 3-step methods. Similar results were obtained in three experiments.

MYPT1 and LC_{20} phosphoprotein levels are increased in pressurized arteries

The effect of pressure and ROK inhibition on the level of MYPT1 and LC_{20} phosphorylation was studied by Western blot analysis. We employed vessel segments with a stable diameter (after ~10 min) following steps from 10 mmHg to 10, 60 or 100 mmHg ± H1152 (0.3 μmol l^{-1}) prior to flash-freezing using the pressure protocol shown in Fig. 5. These pressures were selected as 10 mmHg is the fully relaxed condition and 60 and 100 mmHg are just above the threshold for myogenic contraction and close to the upper physiological limit of pressure of RCAs *in vivo* (Heistad, 2001). A similar pressure protocol was employed for analysis of CPI-17 phosphorylation, except that the vessels were flash frozen at 0.5 or 3 min after pressure elevation based on the rapid increase reported for CPI-17 phosphorylation evoked by agonists (e.g. Dimopoulos *et al.* 2007).

To limit variations in detected MYPT1, CPI-17 and LC_{20} phosphorylation, it was necessary to ensure that the myogenicity of the vessels employed in the analysis was comparable. The magnitude of passive dilatation in zero $[Ca^{2+}]_o$ and, thereby, the extent of active constriction could not be assessed due to flash-freezing. For this reason, vessels not displaying a robust myogenic response during an initial pressure step to 80 mmHg were discarded (see protocol in Fig. 5). Validation of the quality of the vessels was achieved by comparing the mean diameter of each group during the step to 80 mmHg and subsequent steps to 10, 60 or 100 mmHg to the values obtained in assessment of the myogenic response (Fig. 4). The diameters at 80 mmHg for the groups employed in the analysis of ROK inhibition were similar, as indicated in Fig. 6*A* (21–23 vessels per group) and not different from that observed in assessment of the myogenic response (shaded bar; data from Fig. 4*E*). Also, the diameters at 10, 60 and 100 mmHg ± H1152 in Fig. 6*B* were not different from those under identical conditions in the myogenic response experiments (shaded bars; data from Fig. 4*E*). Similar results were obtained for experiments assessing CPI-17 phosphorylation (data not shown). We were confident, therefore, that the myogenic responsiveness of the vessels employed in these experiments was comparable.

Two ROK phosphorylation sites, T697 and T855, were previously identified on MYPT1 (Feng *et al.* 1999; Kawano

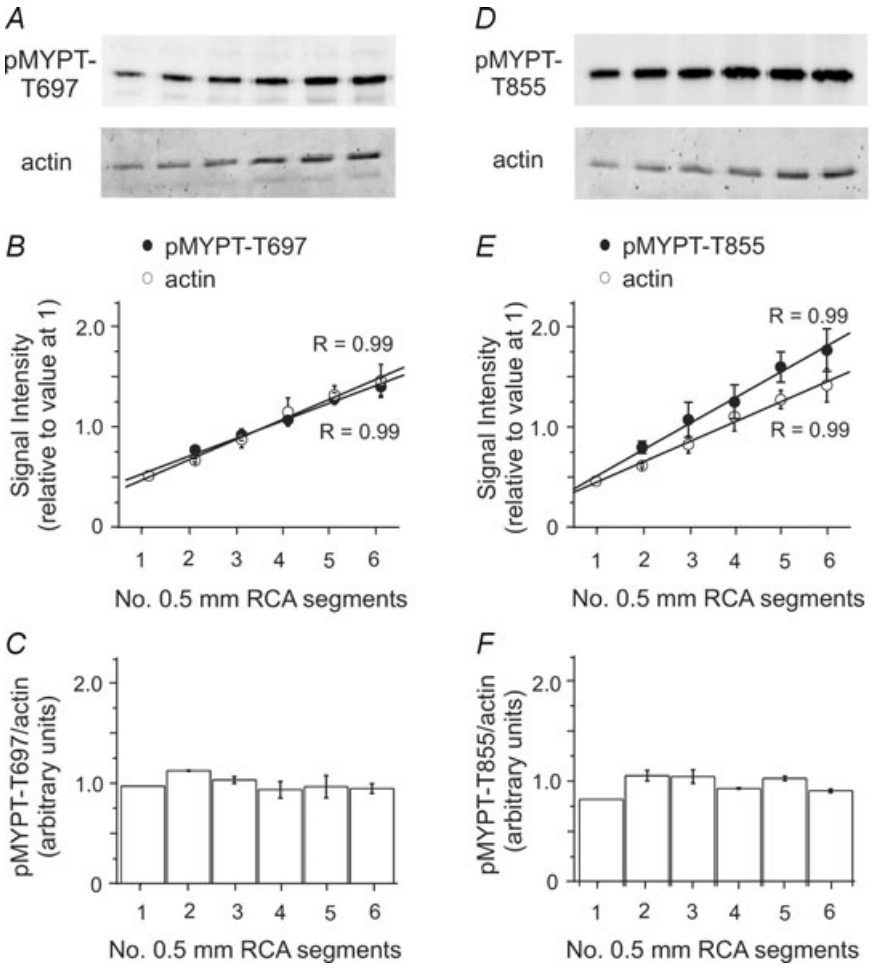

Figure 2. Linearity of phospho-MYPT1-T697 (*A–C*) and phospho-MYPT1-T855 (*D–F*) Western blotting of tissue extracts
A and *D*, dilution series of 10 μmol l^{-1} UTP-stimulated cerebral artery extract was subjected to SDS-PAGE and phosphorylation of MYPT1-T697 and -T855 detected by 3-step Western blotting. *B* and *E*, signal intensity plotted against amount of extract loaded for phospho-T697- and phospho-T855-MYPT1 Western blots, and Coomassie Blue-stained actin, showing the linear relationship between the amount of sample loaded and the detected signal intensity ($n = 3$). *C* and *F*, normalization of the signal intensity of phospho-MYPT1 to Coomassie Blue-stained actin produced a linear relationship that did not deviate from the expected value ($n = 3$).

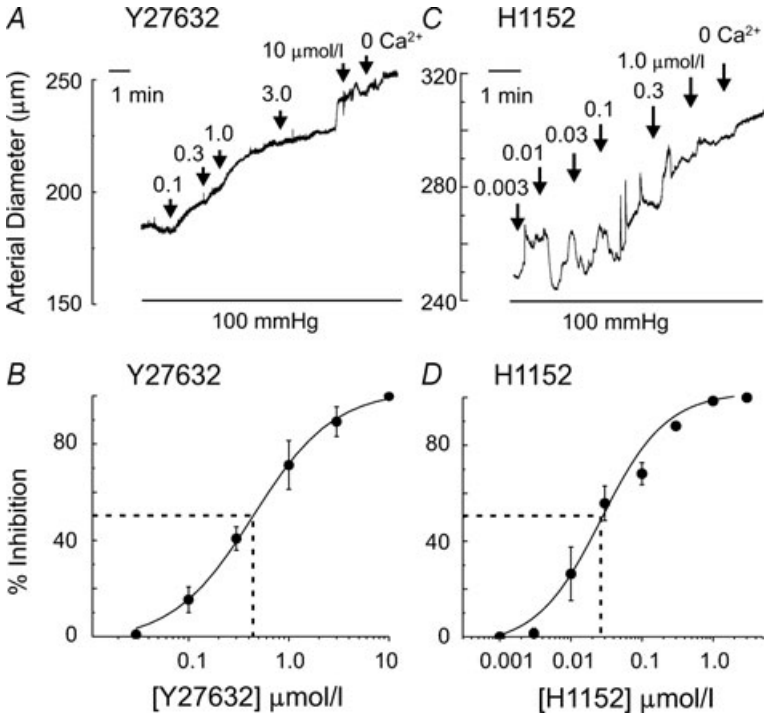

Figure 3. Dilatation of myogenic constriction by ROK inhibition
Representative traces and concentration–response relationships for Y27632- (*A* and *B*; $n = 5$) and H1152-evoked (*C* and *D*; $n = 5$) dilatation at 100 mmHg. Data are expressed as mean ± S.E.M.

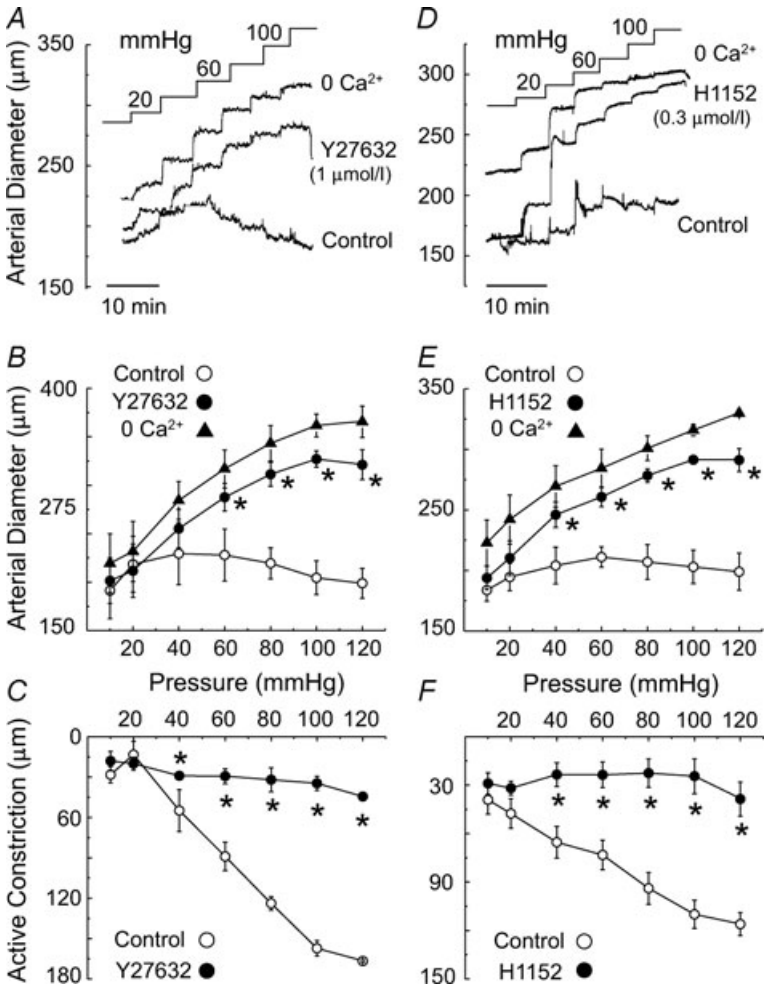

Figure 4. Suppression of the myogenic response by ROK inhibition
Effect of Y27632 (*A*–*C*; $n = 5$) and H1152 (*D*–*F*; $n = 5$) on RCA myogenic response. Representative pressure-induced changes in arterial diameter (*A* and *D*) and mean diameter (± S.E.M.)–pressure relations (*B* and *E*) for 10–120 mmHg in normal Krebs saline (Control), 1 μmol l^{-1} Y27632 or 0.3 μmol l^{-1} H1152, and zero $[Ca^{2+}]_o$ solution, as well as mean active constriction–pressure relations ± Y27632 (*C*) or ± H1152 (*F*). *Significantly different ($P < 0.05$) from control value.

et al. 1999; Velasco *et al.* 2002; Stevenson *et al.* 2004; Murányi *et al.* 2005; Hirano, 2007). Here we employed two phospho-specific, polyclonal antibodies that recognize MYPT1 only when phosphorylated at T697 or T855 (Wilson *et al.* 2005). Figure 7 shows representative Western blots of phospho-MYPT1-T697 and -MYPT1-T855 and the corresponding Coomassie Blue-stained actin content of each sample (6 vessels/lane), as well as the mean ± S.E.M. normalized phosphoprotein as a function of pressure ± H1152 ($n = 3$ blots; protein derived from a total of 16 vessels). At 10 mmHg, RCA exhibited a basal level of MYPT1 phosphorylation at both T697 and T855 (Fig. 7*A*–*D*). The extent of phosphorylation at T855 was significantly increased at 60 and 100 mmHg compared to 10 mmHg (Fig. 7*C* and *D*), but phosphorylation at T697 was not affected by pressure (Fig. 7*A* and *B*). Moreover, both basal (at 10 mmHg) and pressure-induced increases in MYPT1-T855 phosphorylation were significantly reduced by H1152 (Fig. 7*C* and *D*). No change in phospho-MYPT-T697 was observed in the presence of the ROK inhibitor (Fig. 7*A* and *B*).

The pressure-dependent increase in phospho-MYPT1-T855 shown in Fig. 7 would be expected to inhibit MLCP activity and evoke a concurrent H1152-sensitive increase in LC_{20} phosphorylation at 60 and 100 mmHg. Figure 8*A* (6 vessels/lane) shows a representative Western blot of LC_{20} obtained using Phos-tag SDS-PAGE to separate phosphorylated and unphosphorylated protein (Takeya *et al.* 2008). Mono-phosphorylation (1-P) of LC_{20} was apparent, but di-phosphorylation was not detected. Figure 8*B* shows the mean level ± S.E.M. of phosphorylated LC_{20} as a percentage of total LC_{20} protein for 10, 60 and 100 mmHg ± H1152 ($n = 8$ blots; 21–23 vessels total at each pressure). Phosphorylated LC_{20} increased from 24.3 ± 2.6% at 10 mmHg, to 39.3 ± 2.8% and 50.6 ± 3.3% at 60 and 100 mmHg, respectively (Fig. 8*B*). The pressure-dependent increases in LC_{20} phosphorylation at 60 and 100 mmHg were significantly reduced by treatment with H1152.

Inhibition of PKC attenuates myogenic constriction

Figure 9 shows that inhibition of PKC with GF109203X (3 μmol l^{-1}) and Gö6976 (10 μmol l^{-1}) suppressed the myogenic response. The concentrations employed were selected based on their block of agonist-induced contraction (Dimopoulos *et al.* 2007). Vessels were subjected to three series of sequential pressure steps between 20 and 120 mmHg in: (1) control solution, (2) GF109203X ($n = 6$ vessels) or Gö6976 ($n = 6$ vessels), and (3) zero $[Ca^{2+}]_o$ solution. Figure 9 shows that both PKC inhibitors blocked pressure-induced maintenance of arterial diameter and reduced active myogenic constriction.

Pressure does not induce CPI-17 phosphorylation and PKC inhibition does not affect MYPT1 and LC_{20} phosphorylation

Figure 10*A* shows representative immunoblots of CPI-17 and mean ± S.E.M. levels of phospho-CPI-17

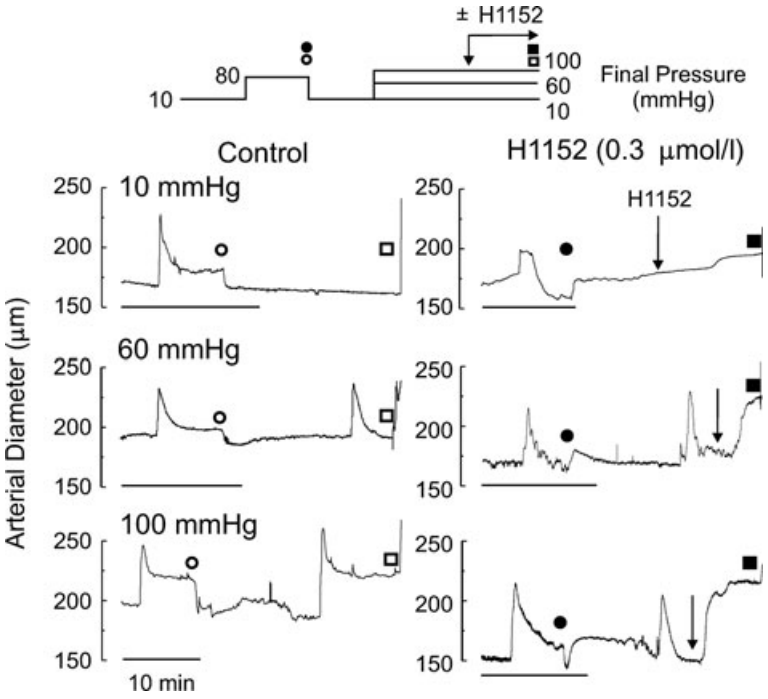

Figure 5. Pressure protocol and representative diameter recordings of arteries used for analysis of MYPT1 and LC_{20} phosphorylation
Representative diameter measurements for a two-pressure-step protocol (top) with common step of 10 to 80 mmHg followed by a step to 10, 60 or 100 mmHg in the absence (Control) or presence of 0.3 μmol l^{-1} H1152 prior to flash-freezing. Scale bars indicate 10 min. Open and filled circles/squares indicate times for diameter measurements in control and H1152 segments, respectively; circles for 80 and squares for 10, 60 or 100 mmHg. CPI-17 analysis used a similar protocol, but tissues were flash-frozen after 3 min at 10, 60 or 100 mmHg. Arrows indicate time of H1152 addition.

in non-pressurized vessels treated with phorbol 12,13-dibutyrate (PdBu; 2 μmol l^{-1}), as well as in pressurized vessels at 10, 60 and 100 mmHg. Unphosphorylated and monophosphorylated CPI-17 were separated by Phos-tag SDS-PAGE (Takeya *et al.* 2008). Treatment with PdBu significantly increased the level of phospho-CPI-17 expressed as a percentage of total CPI-17. However, no change in phospho-CPI-17 was observed at 60 and 100 mmHg compared to 10 mmHg in pressurized arteries (Fig. 10*A*). We also assessed phospho-CPI-17 at an additional time point of 0.5 min after stepping to 100 mmHg to ensure that we had not missed a very rapid change in CPI-17 phosphorylation (Dimopoulos *et al.* 2007). A similar lack of change in phospho-CPI-17 was also detected at this time point (data not shown). We considered the possibility that treatment with PKC inhibitor affected ROK activation leading to altered MYPT1 and LC_{20} phosphorylation. Pairs of vessels from individual rats were pressurized to 100 mmHg prior to treatment with Krebs in the absence or presence of GF109203X (3 μmol l^{-1}) and flash-frozen for determination of phosphoprotein levels. Although the PKC inhibitor induced dilatation, there was no change in the level of LC_{20} ($n = 5$ pairs), MYPT1-T697 ($n = 3$ pairs) or MYPT1-T855 ($n = 3$ pairs) phosphorylation compared to control vessels (Fig. 10*B*–*E*).

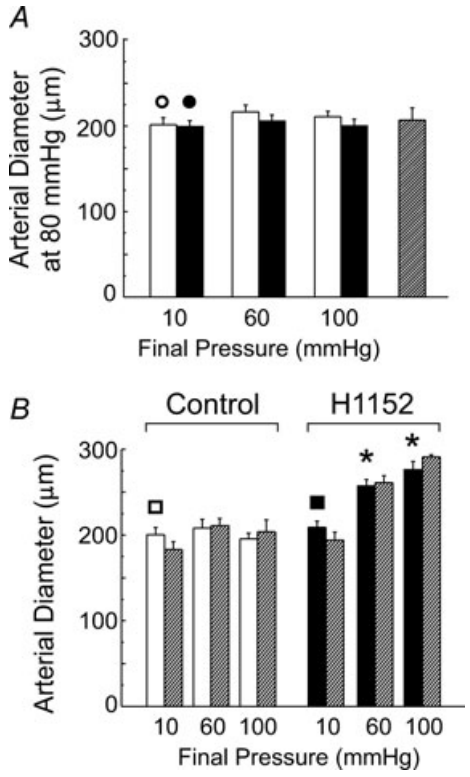

Figure 6. Mean arterial diameters of vessels used for biochemical analysis
A, mean diameter ± S.E.M. for the 10, 60 and 100 mmHg final pressure groups during the initial step to 80 mmHg in Control (open bars) and H1152-containing (black bars) solution (values determined at times indicated in Fig. 5 by open and filled circles, respectively). Shaded bar is mean diameter in control conditions at 80 mmHg (data from Fig. 4). *B*, mean diameter ± S.E.M. prior to flash-freezing at points indicated in Fig. 5 by open and filled squares for control (open bars) and H1152-treated (black bars) arteries, respectively, at 10, 60 and 100 mmHg. Shaded bars are diameters in control and H1152-containing solution at 10, 60 and 100 mmHg (data from Fig. 4). *Significantly different ($P < 0.05$) from value in control solution.

Discussion

This is the first study to quantify MYPT1 and CPI-17 phosphorylation in pressurized true resistance arteries. We provide the first direct, biochemical evidence of ROK-dependent, concurrent changes in the phosphorylation of MYPT1 and LC_{20} in the myogenic response to increased transmural pressure. Our findings were facilitated by the development of a novel, highly sensitive method for the detection and quantification of MYPT1 and CPI-17 phosphorylation in very small samples of protein derived from pressurized RCA (~1 μg protein), similar to that previously used for quantification of phospho-LC_{20} in renal afferent arterioles (Takeya *et al.* 2008). We show that: (1) H1152 suppressed the myogenic constriction in a concentration-dependent manner; (2) myogenic contraction to elevated pressure was associated with a concurrent increase in MYPT1 and LC_{20} phosphorylation that was blocked by H1152; (3) MYPT1 phosphorylation during the myogenic response occurred at T855, but not T697; (4) myogenic contraction was reduced by PKC inhibitors, but there was no change in CPI-17 with increased pressure and pressure-induced MYPT1 and LC_{20} phosphorylation were not affected by PKC inhibitor treatment. These novel findings have important implications for control of arterial diameter by transmural pressure in health and disease.

The ability to simultaneously quantify MYPT1, CPI-17 and LC_{20} phosphorylation in protein samples of less than 1 μg derived from single pressurized resistance arteries represents a significant technical advance. LC_{20} was shown to be phosphorylated to a similar stoichiometry under basal conditions at 10 mmHg and during the myogenic response of RCAs as previously reported for rat cremaster arterioles (Zou *et al.* 1995, 2000). Stretch was previously shown to increase LC_{20} phosphorylation in a ROK-dependent manner in basilar artery (Obara *et al.* 2006), but the involvement of phospho-MYPT1 was not determined. Here, increased MYPT1-T855 and LC_{20} phosphorylation were shown to be associated with myogenic constriction and to be blocked by inhibition of ROK with H1152. A limitation of this study is that ROK and MLCP activities were not measured directly. However, we are confident that both enzymes were activated by

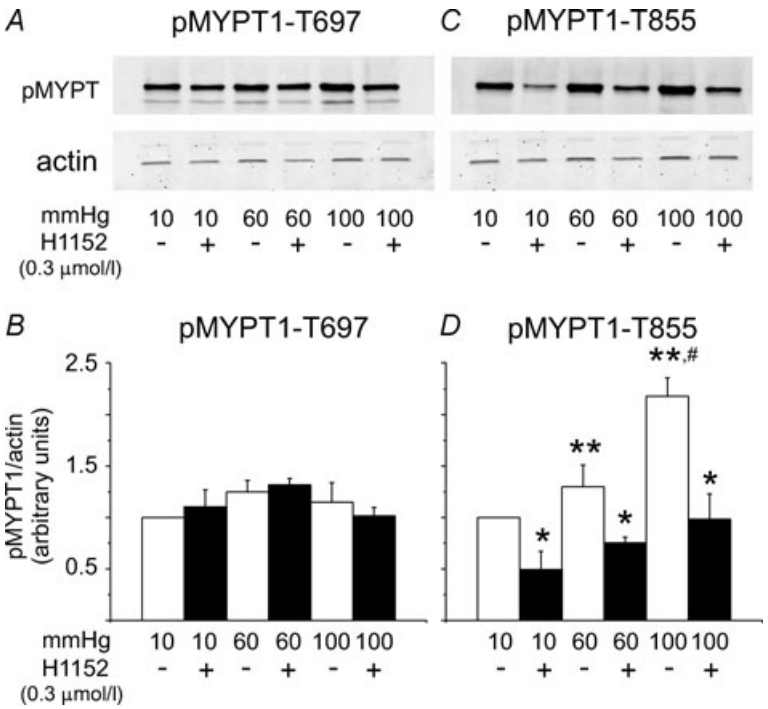

Figure 7. Alteration in MYPT1 phosphorylation with pressure and ROK inhibition
Representative 3-step Western blots of phospho-T697-MYPT1 (*A*) and phospho-T855-MYPT1 (*C*) and corresponding Coomassie-Blue-stained actin level in each lane for samples of arteries at 10, 60 or 100 mmHg ± H1152 (0.3 μmol l^{-1}). *B* and *D* indicate mean level ± S.E.M. ($n = 3$) of phospho-T697- and phospho-T855-MYPT1, respectively, normalized to Coomassie-Blue actin with the value for control at 10 mmHg for each blot set to a value of 1. *Significant difference ($P < 0.05$) from control value at each pressure; **significant difference ($P < 0.05$) from control value at 10 mmHg; #significant difference ($P < 0.05$) from value at 60 mmHg.

pressure based on the following findings. (1) Although Y27632 inhibits PKC (Eto *et al.* 2001; Wilson *et al.* 2005), we found that H1152 reduced myogenic contraction with a 10-fold greater potency than Y27632. This result and the increase in phospho-MYPT1-T855 with pressure elevation are consistent with the involvement of ROK. RhoA translocation to the plasma membrane was also previously shown for myogenic contraction of mesenteric arteries (Dubroca *et al.* 2007). (2) We do not attribute suppression of the myogenic response by H1152 to a decline in $[Ca^{2+}]_i$. Gokina *et al.* (2005) found that ROK inhibition by Y27632 elevated $[Ca^{2+}]_i$ at $>$ 60 mmHg. (3) The complete inhibition of MYPT1 and LC_{20} phosphorylation by H1152 indicates that a change in actin cytoskeleton dynamics (Cipolla & Osol, 1998; Cipolla *et al.* 2002; Gerthoffer, 2005; Corteling *et al.* 2007) is not required to explain the effects of ROK inhibition on pressure-induced force generation. The cytoskeleton may indeed be altered, but the H1152-induced reduction in LC_{20} phosphorylation at 60 and 100 mmHg to the basal level at 10 mmHg can completely account for the loss of myogenic constriction. (4) Coincident changes in phospho-MYPT1, LC_{20} phosphorylation and diameter owing to increased pressure, as well as following treatment with H1152 were detected at 60 and 100 mmHg. This is consistent with a role for pressure-induced MLCP inhibition. LC_{20} phosphorylation at 10 mmHg was not affected by H1152 although the level of phospho-MYPT1-T855 was decreased. This implies that the increase in MLCP activity due to H1152 was insufficient to counteract basal phosphorylation of LC_{20} by MLCK, zipper-interacting protein kinase, p21-activated

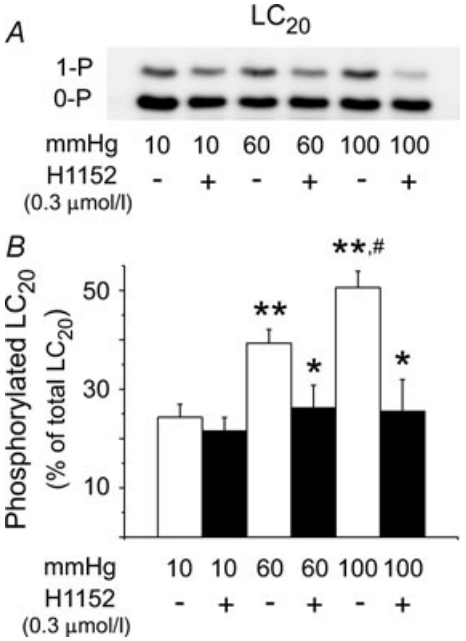

Figure 8. Alteration in LC_{20} phosphorylation with pressure and ROK inhibition
Representative Western blot (*A*) and mean level ± S.E.M. (*B*) of phosphorylated LC_{20} as a percentage of total LC_{20} at 10, 60 and 100 mmHg ± H1152 (0.3 μmol l^{-1}) with unphosphorylated (0-P) and mono-phosphorylated (1-P) LC_{20} separated by Phos-tag SDS-PAGE ($n = 8$). *Significant difference ($P < 0.05$) from control value at each pressure; **significant difference ($P < 0.05$) from control value at 10 mmHg; #significant difference ($P < 0.05$) from value at 60 mmHg.

kinase and/or integrin-linked kinase (Hirano, 2007). Taken together, these data are consistent with the view that increased transmural pressure evokes a ROK-mediated inhibition of MLCP, changing the balance of MLCK-MLCP activity, and permitting net phosphorylation of LC_{20} and increased force generation.

The view that Ca^{2+} sensitization as a result of ROK-mediated phosphorylation of MYPT1 contributes to the myogenic response is consistent with the findings of Gokina *et al.* (2005), but not those of McCarron *et al.* (1997). Gokina *et al.* (2005) observed a reduced sensitivity to Y27632 at 100 *versus* 60 mmHg in α-toxin-permeabilized RCAs. In contrast, McCarron *et al.* (1997) did not detect a change in Ca^{2+} sensitivity with increased pressure over a range of $[Ca^{2+}]_i$ between 0.001 and 60 μmol l^{-1}. However, GTP was not included in the bath solution employed by McCarron *et al.* (1997), precluding activation of the ROK and phospho-MYPT1-dependent mechanism described here. GTP is a requisite co-factor for G-protein-coupled receptor signalling and RhoA activation and is lost from the cytosol through α-toxin pores of permeabilized preparations (Kitazawa *et al.* 1989). $G_{q/11}$-coupled receptors were recently postulated to act as mechano-sensors in the myogenic response of cerebral arteries (Mederos y Schnitzler *et al.* 2008). If this is the case, then GTP may be required at multiple steps in the signalling cascade leading to myogenic contraction.

Our findings indicate that ROK-mediated Ca^{2+} sensitization in response to pressure is exclusively mediated by MYPT1 phosphorylation at T855 in RCAs. Phosphorylation at T697 inhibits MLCP activity (Feng *et al.* 1999) and phosphorylation at T855 interferes with the binding of MYPT1 to myosin (Velasco *et al.* 2002) and inhibits MLCP activity (Murányi *et al.* 2005). The involvement of T855 is consistent with previous studies of agonist-induced, ROK-mediated Ca^{2+} sensitization in which phosphorylation by ROK was reported to occur exclusively at T855 (Kitazawa *et al.* 2003; Stevenson *et al.* 2004; Wilson *et al.* 2005). Phosphorylation at T697 did not change in response to pressure elevation and was not altered by H1152. This indicates that T697 is not an important site for ROK-mediated regulation of pressure-induced vasoconstriction

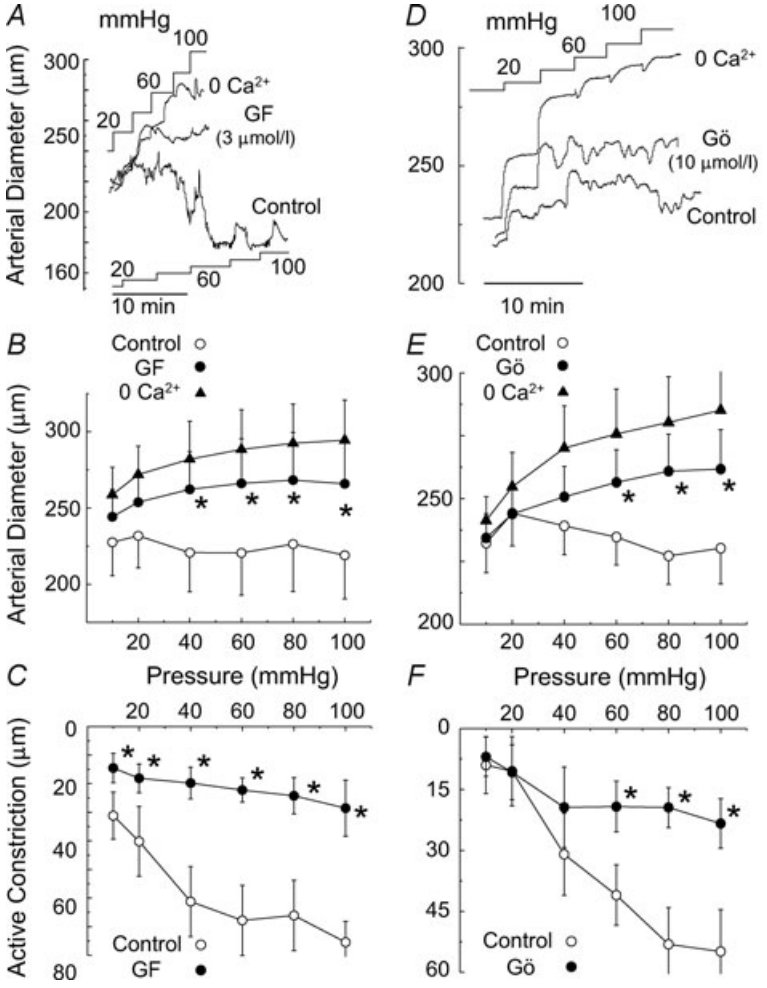

Figure 9. Suppression of the myogenic response by PKC inhibition
Effect of GF109203X (*A–C*; $n = 6$) and Gö6976 (*D–F*; $n = 6$) on RCA myogenic response. Representative pressure-induced changes in arterial diameter (*A* and *D*) and mean diameter (± S.E.M.)–pressure relations (*B* and *E*) for 10–100 mmHg in normal Krebs saline (Control), 3 μmol l^{-1} GF109203X or 10 μmol l^{-1} Gö6976, and zero $[Ca^{2+}]_o$ solution, as well as mean active constriction–pressure relations ± GF109203X (*C*) or ± Gö6976 (*F*). *Significantly different ($P < 0.05$) from control value.

in RCAs. Phosphorylation at T697 is known to occur in response to agonist stimulation (Kitazawa *et al.* 2000; Shin *et al.* 2002; Murthy *et al.* 2003; Niiro *et al.* 2003; Hersch *et al.* 2004; Neppl *et al.* 2009), but not in all preparations or in every instance in which T855 phosphorylation was increased (Kitazawa *et al.* 2003; Stevenson *et al.* 2004; Wilson *et al.* 2005). The kinase responsible for basal phosphorylation at T697 in RCA remains to be determined; potential candidates include zipper-interacting kinase and integrin-linked kinase (MacDonald *et al.* 2001; Murányi *et al.* 2002).

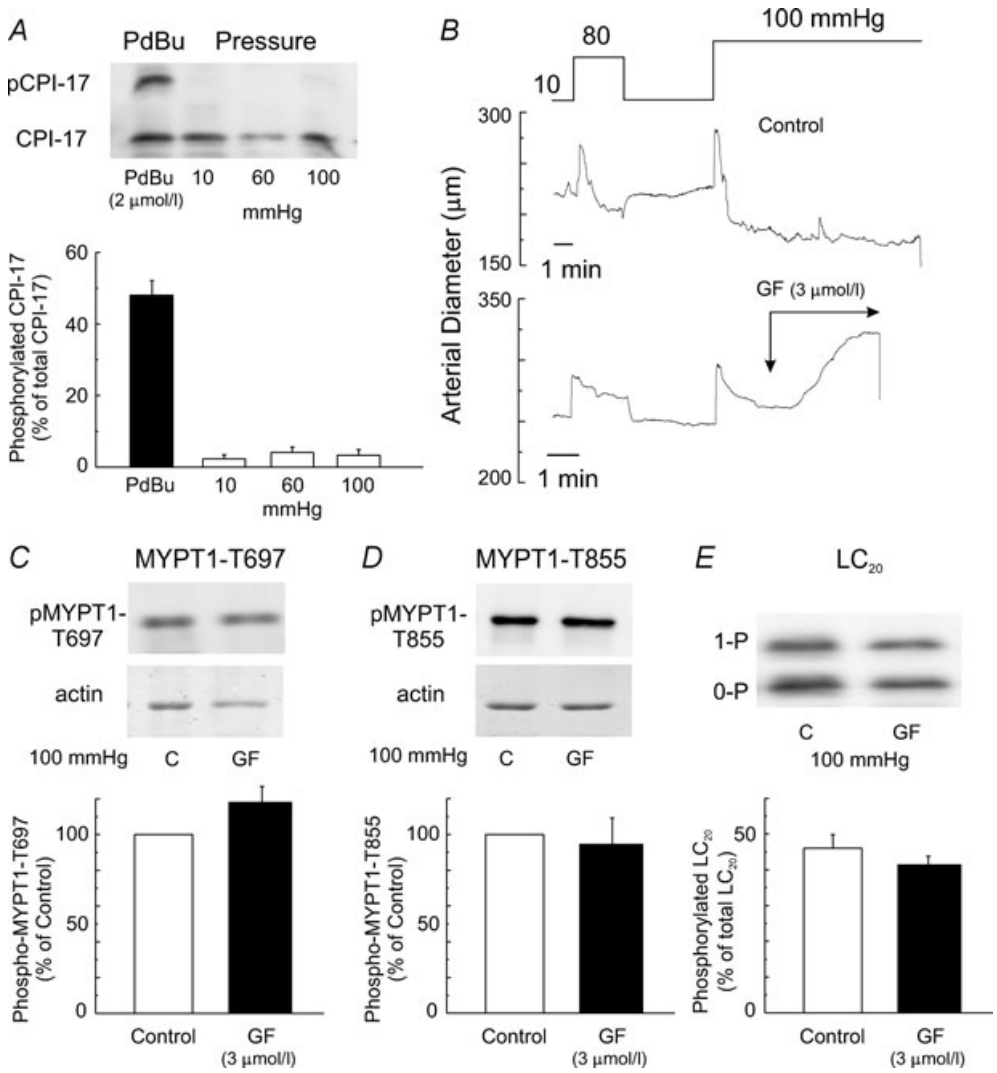

Figure 10. Lack of alteration in CPI-17 phosphorylation with pressure or phospho-MYPT1 and LC_{20} with PKC inhibition

A, representative Western blots and mean level ± S.E.M. of phosphorylated CPI-17 as a percentage of total CPI-17 in arteries treated with PdBu (2 μmol l^{-1}) and arteries at 10, 60 and 100 mmHg with unphosphorylated and phosphorylated CPI-17 separated by Phos-tag SDS-PAGE ($n = 3$). *B*, representative tracings of diameter in response to pressure ± GF109203X (3 μmol l^{-1}; GF) for tissues employed in analysis of CPI-17, MYPT1 and LC_{20} phosphoprotein levels. *C*, representative 3-step Western blots of phospho-MYPT1-T697 and corresponding Coomassie-Blue-stained actin for paired arteries (i.e. both vessels from one rat) at 100 mmHg ± GF109203X (3 μmol l^{-1}; GF) and mean level ± S.E.M. of phospho-T697-MYPT1 in GF109203X-treated vessels ($n = 3$) as a percentage of the level in control conditions ($n = 3$). *D*, representative 3-step Western blots of phospho-MYPT1-T855 and corresponding Coomassie-Blue-stained actin for paired arteries at 100 mmHg ± GF109203X (3 μmol l^{-1}; GF) and mean level ± S.E.M. of phospho-T855-MYPT1 in GF109203X-treated vessels ($n = 3$) as a percentage of the level in control conditions ($n = 3$). *E*, representative 3-step Western blot from paired vessels and mean level ± S.E.M. of phosphorylated LC_{20} as a percentage of total LC_{20} at 100 mmHg ± GF109203X (3 μmol l^{-1}; GF) with unphosphorylated (0-P) and mono-phosphorylated (1-P) LC_{20} separated by Phos-tag SDS-PAGE ($n = 5$ paired arteries in each group).

Our data indicate that PKC-dependent mechanisms of Ca^{2+} sensitization involving CPI-17 and MYPT1 do not contribute to the myogenic response of RCAs. Previous studies using RCAs and other vessels have attributed suppression of the myogenic response by PKC inhibitors to a modulation of Ca^{2+} sensitization (e.g. Karibe *et al.* 1997; Wesselman *et al.* 2001; Lagaud *et al.* 2002; Jarajapu & Knot, 2005). However, this view was based on surrogate markers of sensitization; the effects of pressure and PKC inhibition on CPI-17 and MYPT1 phosphorylation were not determined. PKC-mediated phosphorylation of CPI-17 resulting in Ca^{2+} sensitization is evoked by agonist treatment in several vascular and non-vascular smooth muscles (Eto *et al.* 2001; Dimopoulos *et al.* 2007; Hirano, 2007). For example, GF109203X-sensitive phosphorylation of CPI-17 was observed to reach a peak within 10 s and to slowly decline by ∼25% over 5 min after exposure of femoral arteries to phenylephrine (Dimopoulos *et al.* 2007). Here, we were unable to detect a change in phospho-CPI-17 at 0.5 min (at 100 mmHg) and at 3 min (at 60 and 100 mmHg) after pressure elevation despite reduction of the myogenic response by PKC inhibitor treatment. We do not attribute this negative result to a lack of detection sensitivity or failure to measure phospho-CPI-17 at an appropriate time after pressure elevation. Our approach of 3-step immunoblotting after Phos-tag SDS-PAGE separation of unphosphorylated and phosphorylated CPI-17 was of sufficient sensitivity to resolve a 30% increase in phospho-CPI-17 following treatment with PdBu. Also, arteries were sampled at times consistent with the period of the initial rise in $[Ca^{2+}]_i$, LC_{20} phosphorylation and contraction owing to pressure (Zou *et al.* 1995; D'Angelo *et al.* 1997; Osol *et al.* 2002) and within the period of elevated phospho-CPI-17 following agonist treatment (Dimopoulos *et al.* 2007). PKC inhibitors may block Ca^{2+} sensitization by interfering with RhoA/ROK activation (Kandabashi *et al.* 2003). For example, PKC may phosphorylate RhoGDI leading to dissociation of GDI and RhoA activation by Rho-GEF (Mehta *et al*. 2001). We also failed to identify an effect of GF109203X on MYPT1 or LC_{20} phosphorylation at 100 mmHg. These results provide direct evidence that PKC-dependent Ca^{2+} sensitization via MYPT1 does not contribute to the myogenic response. Also, the lack of change in LC_{20} phosphorylation in the presence of PKC inhibitor implies that a block of PKC-evoked thin filament regulation or cytoskeleton reorganization may be involved rather than a change in ion channel activity, $[Ca^{2+}]_i$ and MLCK activity (McCarron *et al.* 1997; Cipolla & Osol, 1998; Jin *et al.* 2000; Kaneko *et al.* 2000; Morgan & Gangopadhyay 2001; Ghisdal *et al.* 2003; Wier & Morgan, 2003; Shabir *et al.* 2004; Luykenaar *et al.* 2004; Wilson *et al.* 2005; Gerthoffer, 2005; Villalba *et al.* 2008).

Our findings indicate that ROK-mediated inhibition of MLCP is essential for myogenic contraction and suggest the possibility that modulation of pressure-induced ROK activation may be an important site for regulation of myogenic responsiveness. In the absence of MYPT1 phosphorylation due to H1152 treatment, MLCP activity was sufficient to completely suppress pressure-induced LC_{20} phosphorylation and force generation at 60 and 100 mmHg. This implies that pressure-induced myogenic depolarization leading to VGCC activation, Ca^{2+} influx and increased MLCK activity is insufficient to alter the MLCK–MLCP balance to favour LC_{20} phosphorylation and myogenic contraction. Pressure-induced MLCP inhibition by ROK appears to be necessary for the myogenic response to occur in RCAs. Given this essential role for MLCP inhibition, it is significant that the ROK signalling pathway and/or MYPT1 phosphorylation by ROK is suppressed by endothelium-derived nitric oxide and activated by vasoconstrictor agonists (Davis & Hill, 1999; Zou *et al.* 2000; Eto *et al.* 2001; Somlyo & Somlyo, 2003; Swärd *et al.* 2003; Loirand *et al.* 2006; Hirano, 2007; Neppl *et al.* 2009). These factors may alter the level of MLCP inhibition, shifting the phospho-LC_{20}–$[Ca^{2+}]_i$ relation to enhance or suppress myogenic responsiveness without requiring a change in the level of E_m, Ca^{2+} influx or MLCK activation. Osol *et al.* (2002) suggested that the myogenic response may be divided into three distinct phases: myogenic tone development, myogenic reactivity and forced dilatation. Development of myogenic tone between 40 and 60 mmHg is characterized by a substantial depolarization of E_m, elevation in $[Ca^{2+}]_i$ and contraction due to Ca^{2+}–calmodulin-mediated activation of MLCK (Osol *et al.* 2002). However, there is minimal further change in E_m or $[Ca^{2+}]_i$ associated with the myogenic reactivity phase between 60 and 140 mmHg (Osol *et al.* 2002). This implies that Ca^{2+}-dependent increases in MLCK activity have a minor contribution to increased force generation within the physiological range of intra-luminal pressure. Our finding of an H1152-sensitive increase in MYPT1 and LC_{20} phosphorylation between 60 and 100 mmHg indicates that ROK-mediated Ca^{2+} sensitization may play a major role in regulating force generation in the reactivity phase of the myogenic response. Small resistance vessels are permanently exposed to transmural pressure *in vivo* and are in a perpetual state of myogenic activation. The involvement of Ca^{2+} sensitization provides a mechanism to increase force generation with minimal and/or transient increases in $[Ca^{2+}]_i$. This may avoid interference with other Ca^{2+}-dependent processes, minimizing energy expenditure involved in Ca^{2+} homeostasis and precluding toxic effects of prolonged exposure to high $[Ca^{2+}]_i$. Recent findings indicate that pressure elevation evokes Ca^{2+} release from the sarcoplasmic reticulum (SR)

in the form of asynchronous, propagating waves within individual vascular smooth muscle cells (unpublished observations for cremaster arterioles by M. A. Hill and for RCAs by D. G. Welsh), as previously shown for agonist-induced elevations in $[Ca^{2+}]_i$ (e.g. Syyong *et al.* 2009). Presumably, these waves are associated with asynchronous, transient elevations in MLCK activation. MLCP inhibition may be important in this context as it reduces the rate of LC_{20} dephosphorylation. Slowing LC_{20} dephosphorylation would be expected to increase the overlap of asynchronous tone development by individual myocytes due to Ca^{2+} waves and transient MLCK activation leading to greater average force generation within the arterial wall.

The myogenic response is a critical mechanism in cardiovascular physiology and abnormalities in myogenic contraction are well-known to contribute to mortality and morbidity in cardiovascular disease. There is abundant evidence of elevated ROK activity in cardiovascular disorders that are associated with enhanced myogenic responsiveness, such as hypertension (Swärd *et al.* 2003; Jarajapu & Knot, 2005; Loirand *et al.* 2006). The present findings suggest the possibility that this may be due, at least in part, to altered phosphorylation of MYPT1-T855 and increased Ca^{2+} sensitivity. Future application of the 3-step Western blot method described here will provide insights concerning the pressure-dependent signalling pathways that regulate MYPT1 and LC_{20} phosphorylation, as well as permitting quantification of other proteins/phosphoproteins important to resistance arterial function in physiological and pathophysiological conditions.

References

Bayliss WM (1902). On the local reactions of the arterial wall to changes of internal pressure. *J Physiol* **28**, 220–231.

Bolz SS, Vogel L, Sollinger D, Derwand R, Boer C, Pitson SM, Spiegel S & Pohl U (2003). Sphingosine kinase modulates microvascular tone and myogenic responses through activation of RhoA/Rho kinase. *Circulation* **108**, 342–347.

Chen TT, Luykenaar KD, Walsh EJ, Walsh MP & Cole WC (2006). Key role of Kv1 channels in vasoregulation. *Circ Res* **99**, 53–60.

Cipolla MJ, Gokina NI & Osol G (2002). Pressure-induced actin polymerization in vascular smooth muscle as a mechanism underlying myogenic behaviour. *FASEB J* **16**, 72–76.

Cipolla MJ & Osol G (1998). Vascular smooth muscle actin cytoskeleton in cerebral artery forced dilatation. *Stroke* **29**, 1223–1228.

Corteling RL, Brett SE, Yin H, Zheng X-L, Walsh MP & Welsh DG (2007). The functional consequence of RhoA knockdown by RNA interference in rat cerebral arteries. *Am J Physiol Heart Circ Physiol* **293**, H440–H447.

D'Angelo G, Davis MJ & Meininger GA (1997). Calcium and mechanotransduction of the myogenic response. *Am J Physiol Heart Circ Physiol* **273**, H175–H182.

Davis MJ & Hill MA (1999). Signalling mechanisms underlying the vascular myogenic response. *Physiol Rev* **79**, 387–423.

Dimopoulos S, Semba S, Kitazawa K, Eto M, Kitazawa T (2007). Ca^{2+}-dependent rapid Ca^{2+} sensitization of contraction in arterial smooth muscle. *Circ Res* **100**, 121–129.

Dubroca C, Loyer X, Retailleau K, Loirand G, Pacaud P, Feron O, Balligand JL, Levy BI, Heymes C & Henrion D (2007). RhoA activation and interaction with Caveolin-1 are critical for pressure-induced myogenic tone in rat mesenteric resistance arteries. *Cardiovasc Res* **73**, 190–197.

Dubroca C, You D, Levy BI, Loufrani L & Henrion D (2005). Involvement of RhoA/Rho kinase pathway in myogenic tone in the rabbit facial vein. *Hypertension* **45**, 974–979.

Eto M, Kitazawa T, Yazawa M, Mukai H, Ono Y & Brautigan DL (2001). Histamine-induced vasoconstriction involves phosphorylation of a specific inhibitor protein for myosin phosphatase by protein kinase C α and δ isoforms. *J Biol Chem* **276**, 29072–29078.

Feng J, Ito M, Ichikawa K, Isaka N, Nishikawa M, Hartshorne DJ & Nakano T (1999). Inhibitory phosphorylation site for Rho-associated kinase on smooth muscle myosin phosphatase. *J Biol Chem* **274**, 37385–37390.

Gerthoffer WT (2005). Actin cytoskeletal dynamics in smooth muscle contraction. *Can J Physiol Pharmacol* **83**, 851–856.

Ghisdal P, Vandenberg G & Morel N (2003). Rho-dependent kinase is involved in agonist-activated calcium entry in rat arteries. *J Physiol* **551**, 855–867.

Gokina NI, Park KM, McElroy-Yaggy K & Osol G (2005). Effects of Rho kinase inhibition on cerebral artery myogenic tone and reactivity. *J Appl Physiol* **98**, 1940–1948.

Hayashi Y, Senba S, Yazawa M, Brautigan DL & Eto M (2001). Defining the structural determinants and a potential mechanism for inhibition of myosin phosphatase by the protein kinase C-potentiated inhibitor protein of 17 kDa. *J Biol Chem* **276**, 39858–39863.

Heistad DD (2001). What's new in the cerebral microcirculation? Landis Award lecture. *Microcirculation* **8**, 365–375.

Hersch E, Huang J, Grider JR & Murthy KS (2004). G_q/G_{13} signalling by ET-1 in smooth muscle: MYPT1 phosphorylation via ET_A and CPI-17 dephosphorylation via ET_B. *Am J Physiol Cell Physiol* **287**, C1209–C1218.

Hill MA, Davis MJ, Meininger GA, Potocnik SJ & Murphy TV (2006). Arteriolar myogenic signalling mechanisms: Implications for local vascular function. *Clin Hemorheol Microcirc* **34**, 67–79.

Hill MA, Zou H, Potocnik SJ, Meininger GA & Davis MJ (2001). Invited review: arteriolar smooth muscle mechanotransduction: Ca^{2+} signalling pathways underlying myogenic reactivity. *J Appl Physiol* **91**, 973–983.

Hirano K (2007). Current topics in the regulatory mechanism underlying the Ca^{2+} sensitization of the contractile apparatus in vascular smooth muscle. *J Pharmacol Sci* **104**, 109–115.

Jarajapu YP & Knot HJ (2005). Relative contribution of Rho kinase and protein kinase C to myogenic tone in rat cerebral arteries in hypertension. *Am J Physiol Heart Circ Physiol* **289**, H1917–H1922.

Jin JP, Walsh MP, Sutherland C & Chen W (2000). A role for serine-175 in modulating the molecular conformation of calponin. *Biochem J* **350**, 579–588.

Kandabashi T, Shimokawa H, Miyata K, Kunihiro I, Eto Y, Matsumoto Y, Obara K, Nakayama K, Takahashi S & Takeshita A (2003). Evidence for protein kinase C-mediated activation of Rho-kinase in a porcine model of coronary artery spasm. *Arterioscler Thromb Vasc Biol* **23**, 2208–2214.

Kaneko T, Amano M, Maeda A, Goto H, Takahashi K, Ito M & Kaibuchi K (2000). Identification of calponin as a novel substrate of Rho-kinase. *Biochem Biophys Res Commun* **273**, 110–116.

Karibe A, Watanabe J, Horiguchi S, Takeuchi M, Suzuki S, Funakoshi M, Katoh H, Keitoku M, Satoh S & Shirato K (1997). Role of cytosolic Ca^{2+} and protein kinase C in developing myogenic contraction in isolated rat small arteries. *Am J Physiol Heart Circ Physiol* **272**, H1165–H1172.

Kawano Y, Fukata Y, Oshiro N, Amano M, Nakamura T, Ito M, Matsumura F, Inagaki M & Kaibuchi K (1999). Phosphorylation of myosin-binding subunit (MBS) of myosin phosphatase by Rho-kinase *in vivo*. *J Cell Biol* **147**, 1023–1038.

Kitazawa T, Eto M, Woodsome TP & Brautigan DL (2000). Agonists trigger G protein-mediated activation of the CPI-17 inhibitor phosphoprotein of myosin light chain phosphatase to enhance vascular smooth muscle contractility. *J Biol Chem* **275**, 9897–9900.

Kitazawa T, Eto M, Woodsome TP & Khalequzzaman MD (2003). Phosphorylation of the myosin phosphatase targeting subunit and CPI-17 during Ca^{2+} sensitization in rabbit smooth muscle. *J Physiol* **546**, 879–889.

Kitazawa T, Kobayashi S, Horiuti K, Somlyo AV & Somlyo AP (1989). Receptor-coupled, permeabilized smooth muscle. Role of the phosphatidylinositol cascade, G-proteins, and modulation of the contractile response to Ca^{2+}. *J Biol Chem* **264**, 5339–5342.

Lagaud G, Gaudreault N, Moore ED, Van Breemen C & Laher I (2002). Pressure-dependent myogenic constriction of cerebral arteries occurs independently of voltage-dependent activation. *Am J Physiol Heart Circ Physiol* **283**, H2187–2195.

Loirand G, Guilluy C & Pacaud P (2006). Regulation of Rho proteins by phosphorylation in the cardiovascular system. *Trends Cardiovasc Med* **16**, 199–204.

Luykenaar KD, Brett SE, Wu BN & Welsh DG (2004). Pyrimidine nucleotides suppress K_{DR} currents and depolarize rat cerebral arteries by activating Rho kinase. *Am J Physiol Heart Circ Physiol* **286**, H1088–H1100.

McCarron JG, Crichton CA, Langton PD, MacKenzie A & Smith GL (1997). Myogenic contraction by modulation of voltage-dependent calcium currents in isolated rat cerebral arteries. *J Physiol* **498**, 371–379.

MacDonald JA, Borman MA, Murányi A, Somlyo AV, Hartshorne DJ & Haystead TA (2001). Identification of the endogenous smooth muscle phosphatase-associated kinase. *Proc Natl Acad Sci U S A* **98**, 2419–2424.

Mederos y Schnitzler M, Storch U, Meibers S, Nurwakagari P, Breit A, Essin K, Gollasch M & Gudermann T (2008). G_q-coupled receptors as mechanosensors mediating myogenic vasoconstriction. *EMBO J* **27**, 3092–3103.

Mehta D, Rahman A & Malik AB (2001). Protein kinase C-α signals Rho-guanine nucleotide dissociation inhibitor phosphorylation and Rho activation and regulates the endothelial cell barrier function. *J Biol Chem* **276**, 22614–22620.

Morgan KG & Gangopadhyay SG (2001). Invited review: Cross-bridge regulation by thin filament-associated proteins. *J Appl Physiol* **91**, 953–962.

Murányi A, Derkach D, Erdödi F, Kiss A, Ito M & Hartshorne DJ (2005). Phosphorylation of Thr695 and Thr850 on the myosin phosphatase target subunit: inhibitory effects and occurrence in A7r5 cells. *FEBS Lett* **579**, 6611–6615.

Murányi A, MacDonald JA, Deng JT, Wilson DP, Haystead TAJ, Walsh MP, Erdödi F, Kiss E, Wu Y & Hartshorne DJ (2002). Phosphorylation of the myosin phosphatase target subunit by integrin-linked kinase. *Biochem J* **366**, 211–216.

Murthy KS, Zhou H, Grider JR, Brautigan DL, Eto M & Makhlouf GM (2003). Differential signalling by muscarinic receptors in smooth muscle: m_2-mediated inactivation of myosin light chain kinase via G_{i3}, Cdc42/Rac1 and p21-activated kinase 1 pathway, and m_3-mediated MLC_{20} (20 kDa regulatory light chain of myosin II) phosphorylation via Rho-associated kinase/myosin phosphatase targeting subunit 1 and protein kinase C/CPI-17 pathway. *Biochem J* **374**, 145–155.

Nakamura A, Hayashi K, Ozawa Y, Fujiwara K, Okubo K, Kanda T, Wakino S & Saruta T (2003). Vessel- and vasoconstrictor-dependent role of Rho/Rho-kinase in renal microvascular tone. *J Vasc Res* **40**, 244–251.

Neppl RL, Lubomirov LT, Momotani K, Pfitzer G, Eto M & Somlyo AV (2009). Thromboxane A_2-induced bi-directional regulation of cerebral arterial tone. *J Biol Chem* **284**, 6348–6360.

Niiro N, Koga Y & Ikebe M (2003). Agonist-induced changes in the phosphorylation of the myosin-binding subunit of myosin light chain phosphatase and CPI-17, two regulatory factors of myosin light chain phosphatase, in smooth muscle. *Biochem J* **369**, 117–128.

Obara K, Uchino M, Koide M, Yamanaka A & Nakayama K (2006). Stretch-induced triphosphorylation of myosin light chain and myogenic tone in canine basilar artery. *Eur J Pharmacol* **534**, 141–151.

Osol G, Brekke JF, McElroy-Yaggy K & Gokina NI (2002). Myogenic tone, reactivity, and forced dilatation: a three-phase model of *in vitro* arterial myogenic behaviour. *Am J Physiol Heart Circ Physiol* **283**, H2260–H2267.

Plane F, Johnson R, Kerr P, Wiehler W, Thorneloe K, Ishii K, Chen T & Cole W (2005). Heteromultimeric Kv1 channels contribute to myogenic control of arterial diameter. *Circ Res* **96**, 216–224.

Sasaki Y, Suzuki M & Hidaka H (2002). The novel and specific Rho-kinase inhibitor (*S*)-(+)-2-methyl-1-[(4-methyl-5-isoquinoline)sulfonyl]-homopiperazine as a probing molecule for Rho-kinase-involved pathway. *Pharmacol Ther* **93**, 225–232.

Schubert R, Kalentchuk VU & Krien U (2002). Rho kinase inhibition partly weakens myogenic reactivity in rat small arteries by changing calcium sensitivity. *Am J Physiol Heart Circ Physiol* **283**, H2288–H2295.

Schubert R, Lidington D & Bolz SS (2008). The emerging role of Ca^{2+} sensitivity in promoting myogenic vasoconstriction. *Cardiovasc Res* **77**, 8–18.

Shabir S, Borisova L, Wray S & Burdyga T (2004). Rho-kinase inhibition and electromechanical coupling in rat and guinea-pig ureter smooth muscle: Ca^{2+}-dependent and -independent mechanisms. *J Physiol* **560**, 839–855.

Shin HM, Je HD, Gallant C, Tao TC, Hartshorne DJ, Ito M & Morgan KG (2002). Differential association and localization of myosin phosphatase subunits during agonist-induced signal transduction in smooth muscle. *Circ Res* **90**, 546–553.

Somlyo AP & Somlyo AV (2003). Ca^{2+} sensitivity of smooth muscle and nonmuscle myosin II: modulated by G proteins, kinases, and myosin phosphatase. *Physiol Rev* **83**, 1325–1358.

Stevenson AS, Matthew JD, Eto M, Luo S, Somlyo AP & Somlyo AV (2004). Uncoupling of GPCR and RhoA-induced Ca^{2+}-sensitization of chicken amnion smooth muscle lacking CPI-17. *FEBS Lett* **578**, 73–79.

Swärd K, Mita M, Wilson DP, Deng JT, Susnjar M & Walsh MP (2003). The role of RhoA and Rho-associated kinase in vascular smooth muscle contraction. *Curr Hypertens Rep* **5**, 66–72.

Syyong HT, Yang HH, Trinh G, Cheung C, Kuo KH & van Breemen C (2009) Mechanism of asynchronous Ca^{2+} waves underlying agonist-induced contraction in the rat basilar artery. *Br J Pharmacol* **156**, 587–600.

Takeya K, Loutzenhiser K, Shiraishi M, Loutzenhiser R & Walsh MP (2008). A highly sensitive technique to measure myosin regulatory light chain phosphorylation: the first quantification in renal arterioles. *Am J Physiol Renal Physiol* **294**, F1487–F1492.

VanBavel E, Van Der Meulen ET & Spaan JA (2001). Role of Rho-associated protein kinase in tone and calcium sensitivity of cannulated rat mesenteric small arteries. *Exp Physiol* **86**, 585–592.

Velasco G, Armstrong C, Morrice N, Frame S & Cohen P (2002). Phosphorylation of the regulatory subunit of smooth muscle protein phosphatase 1M at Thr850 induces its dissociation from myosin. *FEBS Lett* **527**, 101–104.

Villalba N, Stankevicius E, Simonsen U & Prieto D (2008). Rho kinase is involved in Ca^{2+} entry of rat penile small arteries. *Am J Physiol Heart Circ Physiol* **294**, H1923–H1932.

Wesselman JP, Spaan JA, Van Der Meulen ET & VanBavel E (2001). Role of protein kinase C in myogenic calcium-contraction coupling of rat cannulated mesenteric small arteries. *Clin Exp Pharmacol Physiol* **28**, 848–855.

Wier WG & Morgan KG (2003). α_1-Adrenergic signalling mechanisms in contraction of resistance arteries. *Rev Physiol Biochem Pharmacol* **150**, 91–139.

Wilson DP, Susnjar M, Kiss E, Sutherland C & Walsh MP (2005). Thromboxane A_2-induced contraction of rat caudal arterial smooth muscle involves activation of Ca^{2+} entry and Ca^{2+} sensitization: Rho-associated kinase-mediated phosphorylation of MYPT1 at Thr-855, but not Thr-697. *Biochem J* **389**, 763–774.

Yeon DS, Kim JS, Ahn DS, Kwon SC, Kang BS, Morgan KG & Lee YH (2002). Role of protein kinase C- or RhoA-induced Ca^{2+} sensitization in stretch-induced myogenic tone. *Cardiovasc Res* **53**, 431–438.

Zou H, Ratz PH & Hill MA (1995). Role of myosin phosphorylation and $[Ca^{2+}]_i$ in myogenic reactivity and arteriolar tone. *Am J Physiol Heart Circ Physiol* **269**, H1590–H1596.

Zou H, Ratz PH & Hill MA (2000). Temporal aspects of Ca^{2+} and myosin phosphorylation during myogenic and norepinephrine-induced arteriolar constriction. *J Vasc Res* **37**, 556–567.

Author contributions

All authors contributed to the conception and design of the experiments, analysis and interpretation of the results, and drafting of the manuscript, and have approved the published version of this manuscript.

Disclosures

None.

Acknowledgements

This work was conducted in The Smooth Muscle Research Group at the University of Calgary and was supported by a grant from the Canadian Institutes of Health Research (MOP-10568). R.P.J. was supported by the Alberta Heritage Foundation for Medical Research (AHFMR) and Natural Sciences and Engineering Research Council of Canada. A.F.E. was supported by the AHFMR and Canadian Institutes of Health Research. W.C.C. is the Andrew Family Professor in Cardiovascular Research and M.P.W. is an AHFMR Scientist and recipient of a Canada Research Chair (Tier 1) in Vascular Smooth Muscle Research.